



Published in final edited form as:

J Proteome Res. 2007 June ; 6(6): 2176–2185. doi:10.1021/pr060665l.

Tumor Necrosis Factor- α -and Interleukin-1-Induced Cellular Responses: Coupling Proteomic and Genomic Information

Lee W. Ott[†], Katheryn A. Resing[‡], Alecia W. Sizemore[†], Joshua W. Heyen[†], Ross R. Cocklin[†], Nathan M. Pedrick[§], H. Cary Woods[†], Jake Y. Chen^{||,⊥}, Mark G. Goebel[†], Frank A. Witzmann[§], and Maureen A. Harrington^{*,†}

[†]Department of Biochemistry and Molecular Biology, Indiana University School of Medicine, 635 Barnhill Drive, MS 4053, Indianapolis, Indiana 46202

[‡]Department of Chemistry and Biochemistry, University of Colorado at Boulder, Boulder, Colorado 80309

[§]Department of Cellular and Integrated Physiology, Indiana University School of Medicine, Indianapolis, Indiana 46202

^{||}School of Informatics, Indiana University, Indianapolis, Indiana 46202

[⊥]Department of Computer and Information Science, Purdue University School of Science, Indianapolis, Indiana 46202

Abstract

The pro-inflammatory cytokines, Tumor Necrosis Factor-alpha (TNF α) and Interleukin-1 (IL-1) mediate the innate immune response. Dysregulation of the innate immune response contributes to the pathogenesis of cancer, arthritis, and congestive heart failure. TNF α - and IL-1-induced changes in gene expression are mediated by similar transcription factors; however, TNF α and IL-1 receptor knock-out mice differ in their sensitivities to a known initiator (lipopolysaccharide, LPS) of the innate immune response. The contrasting responses to LPS indicate that TNF α and IL-1 regulate different processes. A large-scale proteomic analysis of TNF α - and IL-1-induced responses was undertaken to identify processes uniquely regulated by TNF α and IL-1. When combined with genomic studies, our results indicate that TNF α , but not IL-1, mediates cell cycle arrest.

Keywords

Tumor Necrosis Factor-alpha; Interleukin-1; Cell Cycle Arrest; Permeability Transition Pore; Protein Interaction Network; Mass Spectrometry; Microarray

Introduction

The innate immune response functions as an important line of defense against pathogenic agents and is an integral component of the wound repair process. Both tumor necrosis factor-alpha (TNF α) and Interleukin-1 (IL-1) are cytokines required for activating the innate immune

© xxxx American Chemical Society

^{*}To whom correspondence should be addressed. mharrin@iupui.edu. Tel: (317) 274-7527, Fax: (317) 274-4686.

Supporting Information Available: Table S1, MSPlus and isoform resolver output; Table S2, proteins with GO terms and protein ratios; Figure S1, reproducibility of spectral counts; Figure S2, GO percentages; Figure S3, GO hierarchy; Figure S4, protein interaction network (<http://www.biochemistry.iu.edu/personnel/Goebel/goeblab/Publications.htm>). This material is available free of charge via the Internet at <http://pubs.acs.org>.

response,¹ mediating the recruitment, activation, and adherence of circulating phagocytic cells (macrophages and neutrophils), and terminating the innate immune response.²⁻⁴ Sustained activation and/or dysregulation of the innate immune response may contribute to the underlying pathology of chronic inflammatory diseases (ulcerative colitis,^{5,6} Crohn's Disease,⁷ and rheumatoid arthritis⁸) and life-threatening complications associated with diabetes⁹ and cancer.¹⁰

In response to activation by either bacterial products (lipopolysaccharide, LPS) or foreign particles, circulating macrophages secrete TNF α , an initiator of the innate immune response. In a paracrine manner, TNF α induces surrounding cells to produce interleukin-8 (to elicit phagocyte recruitment)¹¹ and E-selectin (to promote phagocytic cell adhesion to the surrounding endothelium).¹² Autocrine action by TNF α promotes additional TNF α production¹³ as well as the production and release of IL-1 by macrophages.¹⁴ In a paracrine manner, IL-1 induces the local production of Interleukin-6¹⁵ and the expression of Intercellular Adhesion Molecule-1 (ICAM-1).¹⁶ Together, these and other protein products induced by TNF α and IL-1 mediate the innate immune response and lead to activation of the adaptive immune response.

The TNF α and IL-1 signaling pathways lead to the activation of similar transcription factors (NF- κ B, activator protein-1, AP-1, and CCAAT/enhancer-binding protein beta, C/EBP β). Yet, mice with genetic deletions in TNF α or IL-1 or in their cognate receptors respond differentially to known activators of the innate immune response, such as bacterially derived LPS.^{17,18} Wild-type and type I IL-1 receptor knock-out mice show similar mortality rates to low doses of LPS; while type I TNF α receptor knock-out mice are resistant to low doses of LPS. Data derived from studies with receptor and ligand knock-out mice raise the question as to how TNF α - or IL-1-specific processes are elaborated.

Proteomic and genomic analyses each have the potential to monitor multiple intracellular processes simultaneously. We hypothesized that a large-scale analysis combining proteomic and genomic information would provide insight into processes uniquely regulated by TNF α and IL-1. In this study, we provide proteomic data that in combination with existing genomic data demonstrate that TNF α , but not IL-1, specifically induces a cell cycle arrest. The generation of a protein interaction network provides a model outlining a possible mechanism responsible for the cell cycle arrest.

Methods and Materials

Materials

Cell culture media and supplements were purchased from Invitrogen (Carlsbad, CA). Sample preparation reagents and HPLC solvents were purchased from Sigma-Aldrich (St. Louis, MO). Sequence grade trypsin was purchased from Promega (Madison, WI). Recombinant human TNF α and IL-1 α were purchased from Sigma-Aldrich (St. Louis, MO) and Santa Cruz Biotechnology (Santa Cruz, CA), respectively.

Cell Culture

The 293 human embryonic kidney (293 HEK) cell line immortalized with Epstein-Barr nuclear antigen was maintained in Dulbecco's modified Eagle's media supplemented with 10% fetal bovine serum, penicillin/streptomycin, and glutamine at 37 °C in a 95% air/5% CO₂ mixture.

Preparation of Protein Lysates

In all experiments, cell cultures (grown in 100 mm dishes to 90% confluence) were left untreated or were treated with either recombinant human TNF α (10 ng/mL) or recombinant

human IL-1 α (10 ng/mL) for 6 h. Cell monolayers were washed with ice-cold phosphate-buffered saline (PBS), harvested on ice by scraping with a rubber policeman, and collected by centrifugation (2.3g, 5 min, 4 °C). PBS was removed by aspiration, and cell pellets were flash-frozen in liquid nitrogen and stored at -80 °C.

Protein Isolation

Ice-cold lysis buffer (8 M urea and 100 mM ammonium bicarbonate) and acid-washed glass beads were added to frozen cell pellets followed by thawing on ice. To ensure complete lysis, cell pellets were subjected to 10 cycles of 30 s vortexing followed by 30 s of incubation on ice. Cell lysates were separated from glass beads by piercing a hole in the bottom of a microcentrifuge tube followed by centrifugation to elute the lysates into a fresh microcentrifuge tube. Protein concentrations of the soluble lysates were quantified using a Bradford Assay (Bio-Rad, Hercules, CA). Proteins were reduced with dithiothreitol (40:1 dithiothreitol to protein molar ratio) and alkylated with iodoacetamide (20:1 iodoacetamide to protein molar ratio) to prevent unwanted side reactions involving sulfur atoms on cysteine residues. Excess iodoacetamide was neutralized using L-cysteine (40:1 L-cysteine to protein molar ratio). Reduced, alkylated proteins were then subjected to overnight incubation with trypsin at 37 °C (1:70 trypsin to protein molar ratio). Samples were dried under vacuum and resuspended in mobile phase A [5% acetonitrile (ACN), 0.025% formic acid (FA), and 0.001% heptafluorobutyric acid (HFBA)].

High Performance Liquid Chromatography (HPLC) Conditions

All samples were analyzed using the Paradigm MG4 HPLC system (Michrom Bioresources, Inc.) which allowed for fully automated desalting and two-dimensional (Strong Cation Exchange (SCX) and reverse phase (RP)) separation of complex peptide mixtures. Tryptic peptides were loaded (150 μ g; 50 μ L/min) directly onto a C-18 microtrap (Michrom Bioresources, Inc.) and desalted by flushing the trap with 5 vol of mobile phase A. Peptides were then eluted with 98% ACN/0.025% FA/0.001% HFBA (50 μ L/min) directly onto an SCX microtrap (Michrom Bioresources, Inc.). Increasing concentrations of Ammonium formate (4 mM to 1 M) were used to elute the peptides in a stepwise manner onto a C-8 nanotrap (Michrom Bioresources, Inc.) coupled directly with an analytical C-18 column (100 μ m i.d., 10 cm of resin) with a pulled tip. Peptides were eluted (500 nL/min) using a 95 min gradient of 98% ACN/0.025% FA (5%–50%) and sprayed directly into an LTQ Mass Spectrometer (Thermo Scientific).

Mass Spectrometry and Data Analysis

For each treatment group ($n = 3$), an MS scan (m/z 450–1500; 1 microscan) was collected followed by MS/MS scans on the two most abundant ions from the full scan. Dynamic exclusion duration was set to 4 min with early expiration enabled when the signal-to-noise threshold fell below 2 during four or more consecutive full scans. Default instrument settings for maximum trap fill time and target values were used. Collected MS/MS spectra were searched against the Human IPI database (Version 3.08) using Sequest (v. 27 rev. 12) and Mascot (v. 1.9) packages.¹⁹ Peptide identifications were validated using XCorr and MOWSE score filters set in MSPlus.²⁰ The false discovery rate of peptide identification was determined by searching the Human IPI database with protein sequences that have been reversed.²¹

The spectra for each validated peptide were counted, summed, and used as an estimate of protein abundance. In previous studies, spectral counting has been shown to be a good estimator of protein abundance.²⁰ In this study, spectral counting also showed good reproducibility among treatment group replicates as measured by the correlation coefficient (IL-1: Replicate 1 versus Replicate 2 $r = 0.92$, Replicate 1 versus Replicate 3 $r = 0.76$, Replicate 2 versus Replicate 3 $r = 0.75$; TNF α : Replicate 1 versus Replicate 2 $r = 0.94$, Replicate 1 versus Replicate

3 $r = 0.76$, Replicate 2 versus Replicate 3 $r = 0.77$; Untreated: Replicate 1 versus Replicate 3 $r = 0.88$, Replicate 1 versus Replicate 3 $r = 0.73$, Replicate 2 versus Replicate 3 $r = 0.68$). Two-dimensional plots of replicate versus replicate are shown in Figure S1 in Supporting Information.

MSPlus-validated peptides were grouped into protein groups using IsoformResolver²⁰ (MSPlus and IsoformResolver outputs are presented in Table S1, Supporting Information). Protein \log_2 ratios were determined using spectral counting for each treatment group ($n = 3$),²⁰ and the mean ratios were fit to a normal distribution. Protein ratios that were greater than 2 standard deviations from the sample mean have a p -value < 0.05 and were considered statistically significant. Even though biologically significant proteins may be excluded using this approach, it does provide a means for examining the most pronounced protein level changes induced by TNF α and IL-1.

Gene Ontology (GO) Term Analysis

IPI numbers of proteins that significantly changed in response to either TNF α or IL-1 treatment compared with respective controls were loaded into an MS ACCESS database, along with additional information including protein ratios and statistical confidence. We grouped the proteins according to GO categories, excluding proteins detected in only one treatment group identified with a single peptide. We also calculated the mean TNF α and IL-1 protein differential change ratio for each GO category. Text files containing IPI number, their associated GO identification numbers, and GO terms were downloaded from the Gene Ontology Web site (<http://www.geneontology.org>) and integrated into the MS ACCESS database.

Network Analysis

Saccharomyces cerevisiae homologues to human proteins that changed significantly ($p < 0.05$) upon TNF α or IL-1 treatment were identified using NCBI's Homologene database (<http://www.ncbi.nlm.nih.gov/entrez/query.fcgi?db=Homologene>) and performing additional BlastP analysis.²² Since the yeast and human homologues share common protein interaction and functional domains, the homologues likely interact with similar proteins. Using these homologues, we compiled a human protein interaction database based upon a yeast protein interaction database developed in-house. This database integrates the yeast protein interaction databases from SGD (<ftp://ftp.yeastgenome.org/yeast/>) and BIND (<http://bond.unleashedinformatics.com/>). Our in-house yeast database contains genetic and physical interactions on all characterized ORFs and excludes interactions characterized by experiments with potentially high false-positive rates (i.e., yeast two-hybrid experiments). Here, we used the yeast protein interaction database and transferred this knowledge into human for network analysis primarily due to incomplete publicly available human protein interaction databases. To construct the human protein interaction network, we filtered the protein interaction database to include only proteins among or interacting with differentially changed proteins. To visualize the network, Proteolens (<http://bio.informatics.iupui.edu/Proteolens>), a freely accessible software developed to visualize large protein interaction networks, was used.

Analysis of Gene Expression Omnibus Data Sets (GEO-datasets)

Affymetrix microarray GEOdatasets generated from TNF α (unpublished GDS690, unpublished GDS85223) or IL-1 (GDS64924) treated cell cultures were downloaded from the NCBI Web site (<http://www.pubmed.gov>). The mRNA expression data from each data set were downloaded, normalized using the `justgrma()` function of Bioconductor (<http://www.bioconductor.org>),^{25–27} and fit to a normal distribution to determine statistical significance.

Results and Discussion

Physiological responses to TNF α and IL-1 have been defined using receptor and cytokine knock-out mouse models.^{28–33} On the cellular level, information regarding global responses to pro-inflammatory cytokines has been restricted to inferences based upon the analysis of microarray data.^{23,24,34} To gain a better understanding of the global cellular responses elicited by TNF α and IL-1, proteomic technology was used to define the proteome of TNF α - or IL-1-treated human embryonic kidney cells (293 HEK). Since the 293 HEK cell line is widely used in cytokine research, results gained from our study will be of value to other research laboratories.

Selecting Proteins for further Characterization

Between the three treatment groups (untreated, TNF α , and IL-1), 6585 proteins were validated and quantified. Approximately 55% of the protein identifications were based upon a single peptide (single hit proteins). Single hit proteins may represent low-abundance proteins, proteins with numerous post-translational modifications, and/or contain peptides that ionize weakly during an MS analysis. Despite the potential for obtaining biologically significant information from single hit proteins, the single hit proteins were excluded due to their higher false discovery rate (Figure 1). Assuming the false discovery rate equals the probability of incorrectly identifying single hit proteins, the probability for having all peptides incorrectly identified for proteins with one, two, or three identified peptides was 6%, 0.4%, and 0.02%, respectively. Since the probability associated with incorrectly identifying proteins with two or more peptides is less than 1%, only these proteins were selected for further analysis.

Another approach for lowering the false discovery rate is to choose stricter parameters. Theoretically, the number of correctly identified peptides failing to pass XCorr and Mascot filters will decrease with a lower false discovery rate. If this approach is used, it would be difficult to distinguish between the correct and incorrect peptide identifications, and the number of identified proteins may decrease. By the use of a probability-based two-peptide rule in place of lowering score thresholds, single hit proteins are merely placed aside from the current analysis until later experiments warrant further characterization of these proteins to determine biological significance.

Determining Significant Protein Abundance Changes

Spectral counts of validated peptide identifications used to calculate protein ratios (cytokine-treated versus untreated or IL-1 versus TNF α) serve as a measure of protein abundance providing insight into how the cytokines regulate protein levels. To assess the significance of changes in protein abundance, the protein ratios were fit to a normal distribution. The central limit theorem postulates that the larger a data set is, the more it will tend to approximate a normal distribution.³⁵ As expected, the protein ratios from the IL-1-treated versus untreated (Figure 2A) and the TNF α -treated versus untreated (Figure 2B) data sets approximated a normal distribution. On average, 70% of the protein ratios fell within 1 standard deviation (σ) of the average of the protein ratios within a given treatment group (sample mean), 92% of the ratios fell within 2 σ of the sample mean, and 96% of the ratios fell within 3 σ of the sample mean. When a data set follows a normal distribution, the probability of a protein ratio being significantly different from the sample mean is based upon the number of standard deviations a data point varies from the sample mean (Z-score). Protein ratios were considered significant (p -value < 0.05) if they were more than 2 σ away from the mean (Z-score > 2.0 or Z-score < -2.0). Protein ratios at least 2 σ away from the mean represent proteins that exhibited a 2.27- to 3.41-fold change in response to TNF α and a 2.17- to 3.-20-fold change in response to IL-1 (Table 1).

GO provides a hierarchy for cellular processes that increases in specificity when proceeding to the next level within the hierarchy and is commonly used to annotate proteomic data sets.^{36–38} This hierarchy can be employed to gain a global perspective on the processes regulated by TNF α and IL-1. To begin the analysis, individual proteins from each treatment group were assigned a GO process, and the Z-scores of the proteins assigned a given process were averaged. A significance threshold of 2σ was applied to the averages, because if individual proteins follow a normal distribution, then an average of individual protein Z-scores should also follow a normal distribution. At first glance, it would seem that all processes should be statistically significant when the groups themselves consist of individual ratios that were statistically significant. In this data set, many processes were no longer significant in both cytokine treatment groups once grouped together (Figure 3). For example, the DNA replication GO process group was no longer significant in response to IL-1, because some proteins increased and some proteins decreased. As a result, the process fell below the 2σ threshold. In the TNF α treatment group, all proteins mapped to the DNA replication GO process group showed significant decreases upon TNF α treatment with an average standard deviation for the process of $< -2\sigma$. GO processes that are not statistically significant may be indicative of proteins that are modified (i.e., phosphorylation or ubiquitin) after translation has occurred and may serve as the basis for future studies characterizing post-translational modifications occurring in response to TNF α or IL-1 treatment. On the other hand, statistically significant processes may be indicative of proteins that have protein levels directly regulated by a particular cytokine. Since the purpose of this study was to examine protein levels that significantly changed in response to cytokine treatment, only statistically significant GO processes were further characterized. The number of proteins per GO Term expressed as percentage of the total number of proteins is presented in Figure S2 of Supporting Information. A detailed hierarchy for all processes is shown in Figure S3 of Supporting Information.

TNF α treatment leads to changes in the nuclear processes of DNA replication, mRNA export from nucleus, mRNA processing, nucleosome assembly, and protein import into nucleus (Figure 3A). As cells traverse the G1/S border, activation of E2F occurs which leads to the expression of genes necessary for DNA synthesis. During this period, increases in histone gene expression allow the synthesis of histones in order to package the newly synthesized DNA.³⁹ In response to TNF α , we detected a decrease in DNA replication machinery proteins and an increase in the synthesis of histone variants. The decrease in DNA replication machinery coupled with a shift in chromatin conformation due to changes in nucleosome composition may allow the expression of a distinct subset of genes. The protein levels of DNA replication machinery components (RPA1, RPA3, RFC2, and PCNA) were also significantly decreased upon TNF α treatment (Table 2). TNF α treatment also increased protein levels associated with the GO process nucleosome assembly, including the H2A variant H2A.Z (associated with the opening of chromatin to transcription factors⁴⁰) and macroH2A (associated with CpG methylated DNA and heterochromatin)⁴⁰ (Table S2 in Supporting Information). Decreases in the components of the DNA replication machinery and changes in nucleosome composition elicited by TNF α could prevent S phase activities leading to a cell cycle arrest.

Consistent with inducing a growth arrest response, TNF α significantly decreased cyclin dependent kinase-2 (CDK2) protein levels. Analysis of publicly available microarray data sets also revealed that TNF α significantly decreased cyclin A mRNA levels (Table 2). CyclinA/CDK2 activity is required for cells to move through S phase, while cyclin A/Cdc2 complexes regulate G2 progression.^{41,42} Together, a decrease in cyclin A transcript levels and a decrease in CDK2 protein levels would also inhibit cell cycle progression. Interestingly, the TNF α -induced changes in cell cycle progression appear to be independent of changes in the levels of the cyclin-dependent kinase inhibitors (CDKIs) that mediate cell cycle arrest at various points throughout the cell cycle (Table 2).

TNF α and Induction of Cell Cycle Arrest Mediated by HIF1 α Transcriptional Inactivation

The targets of Hypoxia Inducible Factor 1- α (HIF1 α) include genes involved in cell proliferation, angiogenesis, apoptosis, and metabolism.⁴³ Blocking of cell proliferation occurs in the presence of a HIF1 α pharmacological inhibitor (YC-1).⁴⁴ In our proteomic data sets, mitogen activated protein kinase-1 (MAPK1) and CEBP ζ (a co-activator recruited to promoters by CBP/p300) are significantly decreased upon TNF α treatment (Table 2). MAPK1-mediated HIF1 α phosphorylation has been shown to be essential for the formation of complexes containing HIF1 α and the transcriptional co-activator CBP/p300.⁴³ Thus, the TNF α -mediated decreases in MAPK1 and HIF1 α co-activator protein levels could indicate that TNF α mediates the transcriptional inactivation of HIF1 α .

TNF α and HIF1 α Stabilization

Although TNF α has been shown to inhibit HIF1 α protein degradation under normoxic conditions,⁴⁵ the mechanism for this protein stabilization remains poorly understood. In response to TNF α treatment, cullin-2 (Cul2) protein levels decreased (Table 2). Reduced Cul2 protein levels may stabilize HIF1 α , since following the hydroxylation of HIF1 α by prolyl-hydroxylase under normoxic conditions, Cul2 in complex with Von Hippel-Lindau (VHL) mediates HIF1 α ubiquitin-dependent proteasomal degradation.⁴³ Argininosuccinate lyase (ASL), an enzyme that catalyzes the generation of arginine through the catabolism of argininosuccinate, protein levels increased (compared to IL-1 treatment, Table S2 in Supporting Information). The observed increased protein levels of ASL may lead to an increase in intracellular arginine levels, a precursor for nitric oxide.⁴⁶ Since nitric oxide acts as an inhibitor of prolyl-hydroxylase, inhibition of HIF1 α hydroxylation may occur.⁴⁷ Thus, on the basis of our observations, TNF α may stabilize HIF1 α by inducing ASL-mediated prolyl-hydroxylase inactivation and by decreasing Cul2 protein levels.

IL-1 Induced Processes Occurred Mainly in the Cytoplasm

IL-1-induced changes in the processes of ER to Golgi vesicle-mediated transport, glycolysis, microtubule-based movement, mitochondrial transport, protein polymerization, response to unfolded protein, RNA splicing, and ubiquitin-dependent protein catabolism (Figure 3B). IL-1 treatment leads to a significant increase in enzymes that act in concert to raise intracellular pyruvate levels including pyruvate kinase (PKM2; Table 2), phosphoglucomutase (PGM1, Table S2 in Supporting Information) and increases triosephosphate isomerase-1 (TPI1) protein levels (Table 2).

TNF α and IL-1-Induced Metabolic Changes and Differential Regulation of HIF1 α

Exogenous addition of pyruvate and lactate has been shown to stabilize levels of HIF1 α protein through an uncharacterized mechanism.⁴⁸ TNF α treatment significantly increased the protein levels of lactate dehydrogenase (LDHLA6B) (compared to IL-1 treatment, Table S2 in Supporting Information) and the E2 of pyruvate dehydrogenase (DLAT) (compared to the untreated, Table 2). LDHLA6B stimulates the conversion of pyruvate to lactate, while DLAT converts pyruvate to acetyl-CoA.^{49,50} On the basis of our proteomic data, TNF α -induced increases in LDHLA6B and DLAT could increase lactate production, which in turn might also lead to HIF1 α stabilization (Figure 4A).

Studies with 293 HEK cells have shown that the addition of pyruvate leads to accumulation of HIF1 α protein and induces the expression of HIF1 α -dependent genes.⁴⁸ In contrast to the significant increases found in response to TNF α , IL-1 treatment did not lead to changes in the protein levels of DLAT or LDHLA6B (enzymes that catabolize pyruvate) (Table S2 in Supporting Information). Instead, IL-1 treatment leads to an increase in PKM2, which catalyzes

the conversion of phosphoenolpyruvate to pyruvate. Both PKM2, and its product pyruvate have been linked to activation of HIF1 α dependent genes⁴³ (Figure 4).

TNF α and the Regulation of the Mitochondrial Permeability Transition Pore (PTP)

The PTP consists of the following proteins: adenine nucleotide translocase (ANT), voltage-dependent anion channel (VDAC), cyclophilin-D (PPIF), protein transporter at the outer membrane (TOMM40), and protein transporter of the inner membrane (TIMM9).⁵¹ PTP opening allows the entry of small molecules into the lumen of the mitochondria which leads to mitochondrial swelling from osmosis and mitochondrial release of cytochrome C (CytC).⁵² TNF α treatment increased TIMM9 protein levels, while TNF α and IL-1 decreased TOMM40 protein levels. TNF α and IL-1 treatments led to a significant increase in the level of PPIF protein, while TNF α increased PPIF transcript levels to a greater extent than IL-1 (Table 2). The necessity of PPIF and other PTP complex members for PTP opening is under debate. However, PPIF has been shown to protect cells from apoptosis resulting from the opening of the PTP.⁵³ Thus, the increased levels of PPIF protein and transcript may protect against TNF α -induced apoptosis during cell cycle arrest.

Network Analysis Couples PTP and HIF1 α Regulation

A protein interaction network, based upon biochemical and genetic interactions in *S. cerevisiae* (described in Materials and Methods), was used to explore the interactions between HIF1 α and PTP regulatory elements (Figure 5). Upon TNF α treatment, ARD1A, the human homologue of the protein Arrest Defective (ARD1), which is essential for entry into the stationary phase of *S. cerevisiae*,⁵⁴ was increased (Table 2). Mouse studies have shown that under normoxic conditions ARD1A-mediated acetylation of HIF1 α on lysine 532 targets HIF1 α in a VHL/Cul2-dependent manner for proteasomal degradation.⁵⁵ In human cell lines, ARD1A/HIF1 α complexes can be detected; however, loss of ARD1A had no effect upon HIF1 α protein stability.^{56,57} It would appear that ARD1A and HIF1 α proteins may be linked, however, their role in ARD1A activity in the regulation of HIF1 α stability remains unclear.

Conclusion

TNF α production often precedes the production of IL-1 during the innate immune response.¹ In 293 HEK cells, TNF α may prepare the cell to respond to IL-1 through the induction of G1 cell cycle arrest and inhibition of DNA replication. We can formulate a model in which TNF α -mediated cell cycle arrest appears to result from TNF α -dependent increases in lactate leading to stabilization of HIF1 α . IL-1 appears to activate HIF1 α through the induction of glycolytic enzymes that produce pyruvate. The TNF α -induced stabilization of HIF1 α followed by the IL-1 dependent activation of HIF1 α provides an example of how TNF α and IL-1 work together to coordinate different cellular processes to regulate the inflammatory process.

Results from this study demonstrate how a combined examination of both mRNA expression data and proteomic data can provide novel insight into the cellular processes uniquely regulated by TNF α . Data generated in this study provide a starting point for future studies aimed at examining the relationship between the cytokines TNF α and IL-1 in the regulation of the inflammatory response.

Acknowledgments

This research was supported in part by an appointment to the Research Participation Program at the Air Force Research Laboratory, Human Effectiveness Directorate, Bioscience and Protection, Wright-Patterson AFB administered by the Oak Ridge Institute for Science and Education through an interagency agreement between the U.S. Department of Energy and AFRL/HEP, and Indiana University-Purdue University Indianapolis Roadmap Initiative Grant provided

to Drs. Jake Chen, Mark Goebel, and Maureen Harrington. We thank the Goebel lab for use of the yeast protein interaction database and Jake Chen for guidance in the use of Proteolens and the analysis of the microarray data.

References

- Dinarello CA. Proinflammatory cytokines. *Chest* 2000;118(2):503–508. [PubMed: 10936147]
- Kwon HJ, Breese EH, Vig-Varga E, Luo Y, Lee Y, Goebel MG, Harrington MA. Tumor necrosis factor alpha induction of NF-kappaB requires the novel coactivator SIMPL. *Mol. Cell. Biol* 2004;24(21):9317–9326. [PubMed: 15485901]
- Vig E, Green M, Liu Y, Yu KY, Kwon HJ, Tian J, Goebel MG, Harrington MA. SIMPL is a tumor necrosis factor-specific regulator of nuclear factor-kappaB activity. *J. Biol. Chem* 2001;276(11):7859–7866. [PubMed: 11096118]
- Vig E, Green M, Liu Y, Donner DB, Mukaida N, Goebel MG, Harrington MA. Modulation of tumor necrosis factor and interleukin-1-dependent NF-kappaB activity by mPLK/IRAK. *J. Biol. Chem* 1999;274(19):13077–13084. [PubMed: 10224059]
- Bai AP, Ouyang Q, Xiao XR, Li SF. Probiotics modulate inflammatory cytokine secretion from inflamed mucosa in active ulcerative colitis. *Int. J. Clin. Pract* 2006;60(3):284–288. [PubMed: 16494642]
- Li JH, Yu JP, Yu HG, Xu XM, Yu LL, Liu J, Luo HS. Melatonin reduces inflammatory injury through inhibiting NF-kappaB activation in rats with colitis. *Mediators Inflammation* 2005;2005(4):185–193.
- Monteleone G, Fina D, Caruso R, Pallone F. New mediators of immunity and inflammation in inflammatory bowel disease. *Curr. Opin. Gastroenterol* 2006;22(4):361–364. [PubMed: 16760750]
- Cohen SB. The use of anakinra, an interleukin-1 receptor antagonist, in the treatment of rheumatoid arthritis. *Rheum. Dis. Clin. North. Am* 2004;30(2):365–380. vii. [PubMed: 15172046]
- Gonzalez-Gay MA, De Matias JM, Gonzalez-Juanatey C, Garcia-Porrúa C, Sanchez-Andrade A, Martin J, Llorca J. Anti-tumor necrosis factor-alpha blockade improves insulin resistance in patients with rheumatoid arthritis. *Clin. Exp. Rheumatol* 2006;24(1):83–86. [PubMed: 16539824]
- Yoshimura A. Signal transduction of inflammatory cytokines and tumor development. *Cancer Sci* 2006;97(6):439–447. [PubMed: 16734720]
- Yao PL, Lin YC, Wang CH, Huang YC, Liao WY, Wang SS, Chen JJ, Yang PC. Autocrine and paracrine regulation of interleukin-8 expression in lung cancer cells. *Am. J. Respir. Cell Mol. Biol* 2005;32(6):540–547. [PubMed: 15746434]
- Hermosilla C, Zahner H, Taubert A. *Eimeria bovis* modulates adhesion molecule gene transcription in and PMN adhesion to infected bovine endothelial cells. *Int. J. Parasitol* 2006;36(4):423–431. [PubMed: 16500654]
- Hoffmann G, Schloesser M, Czechowski M, Schobersberger W, Furhapter C, Sepp N. Tumor necrosis factor-alpha gene expression and release in cultured human dermal microvascular endothelial cells. *Exp. Dermatol* 2004;13(2):113–119. [PubMed: 15009105]
- Haddad JJ. Recombinant TNF-alpha mediated regulation of the I kappa B-alpha/NF-kappa B signaling pathway: evidence for the enhancement of pro- and anti-inflammatory cytokines in alveolar epithelial cells. *Cytokine* 2002;17(6):301–310. [PubMed: 12061837]
- Ng EK, Panesar N, Longo WE, Shapiro MJ, Kaminski DL, Tolman KC, Mazuski JE. Human intestinal epithelial and smooth muscle cells are potent producers of IL-6. *Mediators Inflammation* 2003;12(1):3–8.
- Hebert MJ, Gullans SR, Mackenzie HS, Brady HR. Apoptosis of endothelial cells is associated with paracrine induction of adhesion molecules: evidence for an interleukin-1beta-dependent paracrine loop. *Am. J. Pathol* 1998;152(2):523–532. [PubMed: 9466579]
- Glaccum MB, Stocking KL, Charrier K, Smith JL, Willis CR, Maliszewski C, Livingston DJ, Peschon JJ, Morrissey PJ. Phenotypic and functional characterization of mice that lack the type I receptor for IL-1. *J. Immunol* 1997;159(7):3364–3371. [PubMed: 9317135]
- Rothe J, Lesslauer W, Lotscher H, Lang Y, Koebel P, Kontgen F, Althage A, Zinkernagel R, Steinmetz M, Bluethmann H. Mice lacking the tumour necrosis factor receptor 1 are resistant to TNF-mediated toxicity but highly susceptible to infection by *Listeria monocytogenes*. *Nature* 1993;364(6440):798–802. [PubMed: 8395024]

19. Sun S, Meyer-Arendt K, Eichelberger B, Brown R, Yen CY, Old WM, Pierce K, Cios KJ, Ahn NG, Resing KA. Improved validation of peptide MS/MS assignments using spectral intensity prediction. *Mol. Cell. Proteomics* 2007;6(1):1–17. [PubMed: 17018520]
20. Old WM, Meyer-Arendt K, Aveline-Wolf L, Pierce KG, Mendoza A, Sevinsky JR, Resing KA, Ahn NG. Comparison of label-free methods for quantifying human proteins by shotgun proteomics. *Mol. Cell. Proteomics* 2005;4(10):1487–1502. [PubMed: 15979981]
21. Resing KA, Meyer-Arendt K, Mendoza AM, Aveline-Wolf LD, Jonscher KR, Pierce KG, Old WM, Cheung HT, Russell S, Wattawa JL, Goehle GR, Knight RD, Ahn NG. Improving reproducibility and sensitivity in identifying human proteins by shotgun proteomics. *Anal. Chem* 2004;76(13):3556–3568. [PubMed: 15228325]
22. Altschul SF, Gish W, Miller W, Myers EW, Lipman DJ. Basic local alignment search tool. *J. Mol. Biol* 1990;215(3):403–410. [PubMed: 2231712]
23. dos Santos CC, Han B, Andrade CF, Bai X, Uhlig S, Hubmayr R, Tsang M, Lodyga M, Keshavjee S, Slutsky AS, Liu M. DNA microarray analysis of gene expression in alveolar epithelial cells in response to TNFalpha, LPS, and cyclic stretch. *Physiol. Genomics* 2004;19(3):331–342. [PubMed: 15454581]
24. Mayer H, Bilban M, Kurtev V, Gruber F, Wagner O, Binder BR, de Martin R. Deciphering regulatory patterns of inflammatory gene expression from interleukin-1-stimulated human endothelial cells. *Arterioscler., Thromb., Vasc. Biol* 2004;24(7):1192–1198. [PubMed: 15130917]
25. Irizarry RA, Hobbs B, Collin F, Beazer-Barclay YD, Antonellis KJ, Scherf U, Speed TP. Exploration, normalization, and summaries of high density oligonucleotide array probe level data. *Biostatistics* 2003;4(2):249–264. [PubMed: 12925520]
26. Irizarry RA, Bolstad BM, Collin F, Cope LM, Hobbs B, Speed TP. Summaries of Affymetrix GeneChip probe level data. *Nucleic Acids Res* 2003;31(4):e15. [PubMed: 12582260]
27. Bolstad BM, Irizarry RA, Astrand M, Speed TP. A comparison of normalization methods for high density oligonucleotide array data based on variance and bias. *Bioinformatics* 2003;19(2):185–193. [PubMed: 12538238]
28. Mizgerd JP, Spieker MR, Doerschuk CM. Early response cytokines and innate immunity: essential roles for TNF receptor 1 and type I IL-1 receptor during *Escherichia coli* pneumonia in mice. *J. Immunol* 2001;166(6):4042–4048. [PubMed: 11238652]
29. Moore RJ, Owens DM, Stamp G, Arnott C, Burke F, East N, Holdsworth H, Turner L, Rollins B, Pasparakis M, Kollias G, Balkwill F. Mice deficient in tumor necrosis factor-alpha are resistant to skin carcinogenesis. *Nat. Med* 1999;5(7):828–831. [PubMed: 10395330]
30. Amiot F, Fitting C, Tracey KJ, Cavaillon JM, Dautry F. Lipopolysaccharide-induced cytokine cascade and lethality in LT alpha/TNF alpha-deficient mice. *Mol. Med* 1997;3(12):864–875. [PubMed: 9440119]
31. Fantuzzi G, Dinarello CA. The inflammatory response in interleukin-1 beta-deficient mice: comparison with other cytokine-related knock-out mice. *J. Leukocyte Biol* 1996;59(4):489–493. [PubMed: 8613694]
32. Kozak W, Kluger MJ, Soszynski D, Conn CA, Rudolph K, Leon LR, Zheng H. IL-6 and IL-1 beta in fever. Studies using cytokine-deficient (knockout) mice. *Ann. N. Y. Acad. Sci* 1998;856:33–47. [PubMed: 9917862]
33. Rudolph D, Yeh WC, Wakeham A, Rudolph B, Nallainathan D, Potter J, Elia AJ, Mak TW. Severe liver degeneration and lack of NF-kappaB activation in NEMO/IKKgamma-deficient mice. *Genes Dev* 2000;14(7):854–862. [PubMed: 10766741]
34. Anderle P, Rumbo M, Siervo F, Mansourian R, Michetti P, Roberts MA, Kraehenbuhl JP. Novel markers of the human follicle-associated epithelium identified by genomic profiling and microdissection. *Gastroenterology* 2005;129(1):321–327. [PubMed: 16012957]
35. Johnson, O. *Information Theory and the Central Limit Theorem*. London: Imperial College Press; 2004.
36. Ahn WS, Kim KW, Bae SM, Yoon JH, Lee JM, Namkoong SE, Kim JH, Kim CK, Lee YJ, Kim YW. Targeted cellular process profiling approach for uterine leiomyoma using cDNA microarray, proteomics and gene ontology analysis. *Int. J. Exp. Pathol* 2003;84(6):267–279. [PubMed: 14748746]

37. Blonder J, Terunuma A, Conrads TP, Chan KC, Yee C, Lucas DA, Schaefer CF, Yu LR, Issaq HJ, Veenstra TD, Vogel JC. A proteomic characterization of the plasma membrane of human epidermis by high-throughput mass spectrometry. *J. Invest. Dermatol* 2004;123(4):691–699. [PubMed: 15373774]
38. Ruth MC, Old WM, Emrick MA, Meyer-Arendt K, Aveline-Wolf LD, Pierce KG, Mendoza AM, Sevinsky JR, Hamady M, Knight RD, Resing KA, Ahn NG. Analysis of membrane proteins from human chronic myelogenous leukemia cells: comparison of extraction methods for multidimensional LC–MS/MS. *J. Proteome Res* 2006;5(3):709–719. [PubMed: 16512687]
39. Stein GS, van Wijnen AJ, Stein JL, Lian JB, Montecino M, Zaidi SK, Braastad C. An architectural perspective of cell-cycle control at the G1/S phase cell-cycle transition. *J. Cell. Physiol* 2006;209(3):706–710. [PubMed: 17001681]
40. Bernstein E, Hake SB. The nucleosome: a little variation goes a long way. *Biochem. Cell Biol* 2006;84(4):505–517. [PubMed: 16936823]
41. Kaldis P, Aleem E. Cell cycle sibling rivalry: Cdc2 vs. Cdk2. *Cell Cycle* 2005;4(11):1491–1494. [PubMed: 16258277]
42. Yam CH, Fung TK, Poon RY. Cyclin A in cell cycle control and cancer. *Cell. Mol. Life Sci* 2002;59(8):1317–1326. [PubMed: 12363035]
43. Ke Q, Costa M. Hypoxia-inducible Factor-1 (HIF-1). *Mol. Pharmacol* 2006;70(5):1469–1480. [PubMed: 16887934]
44. Yeo EJ, Ryu JH, Chun YS, Cho YS, Jang IJ, Cho H, Kim J, Kim MS, Park JW. YC-1 induces S cell cycle arrest and apoptosis by activating checkpoint kinases. *Cancer Res* 2006;66(12):6345–6352. [PubMed: 16778212]
45. Zhou J, Schmid T, Brune B. Tumor necrosis factor- α causes accumulation of a ubiquitinated form of hypoxia inducible factor-1 α through a nuclear factor- κ B-dependent pathway. *Mol. Biol. Cell* 2003;14(6):2216–2225. [PubMed: 12808024]
46. Wu G, Morris SM Jr. Arginine metabolism: nitric oxide and beyond. *Biochem. J* 1998;336(Pt. 1):1–17. [PubMed: 9806879]
47. Metzzen E, Zhou J, Jelkmann W, Fandrey J, Brune B. Nitric oxide impairs normoxic degradation of HIF-1 α by inhibition of prolyl hydroxylases. *Mol. Biol. Cell* 2003;14(8):3470–3481. [PubMed: 12925778]
48. Lu H, Forbes RA, Verma A. Hypoxia-inducible factor 1 activation by aerobic glycolysis implicates the Warburg effect in carcinogenesis. *J. Biol. Chem* 2002;277(26):23111–23115. [PubMed: 11943784]
49. Perham RN. Swinging arms and swinging domains in multifunctional enzymes: catalytic machines for multistep reactions. *Annu. Rev. Biochem* 2000;69:961–1004. [PubMed: 10966480]
50. Adams MJ, Buehner M, Chandrasekhar K, Ford GC, Hackert ML, Liljas A, Rossmann MG, Smiley IE, Allison WS, Everse J, Kaplan NO, Taylor SS. Structure-function relationships in lactate dehydrogenase. *Proc. Natl. Acad. Sci. U.S.A* 1973;70(7):1968–1972. [PubMed: 4146647]
51. Forte M, Bernardi P. Genetic dissection of the permeability transition pore. *J. Bioenerg. Biomembr* 2005;37(3):121–128. [PubMed: 16167169]
52. Lee WK, Bork U, Gholamrezaei F, Thevenod F. Cd(2+)-induced cytochrome c release in apoptotic proximal tubule cells: role of mitochondrial permeability transition pore and Ca-(2+) uniporter. *Am. J. Physiol.: Renal Physiol* 2005;288(1):F27–F39. [PubMed: 15339793]
53. Tsujimoto Y, Nakagawa T, Shimizu S. Mitochondrial membrane permeability transition and cell death. *Biochim. Biophys. Acta.* 2006
54. Mullen JR, Kayne PS, Moerschell RP, Tsunasawa S, Gribskov M, Colavito-Shepanski M, Grunstein M, Sherman F, Sternglanz R. Identification and characterization of genes and mutants for an N-terminal acetyltransferase from yeast. *EMBO J* 1989;8(7):2067–2075. [PubMed: 2551674]
55. Jeong JW, Bae MK, Ahn MY, Kim SH, Sohn TK, Bae MH, Yoo MA, Song EJ, Lee KJ, Kim KW. Regulation and destabilization of HIF-1 α by ARD1-mediated acetylation. *Cell* 2002;111(5):709–720. [PubMed: 12464182]
56. Arnesen T, Kong X, Evjenth R, Gromyko D, Varhaug JE, Lin Z, Sang N, Caro J, Lillehaug JR. Interaction between HIF-1 α (ODD) and hARD1 does not induce acetylation and destabilization of HIF-1 α . *FEBS Lett* 2005;579(28):6428–6432. [PubMed: 16288748]

57. Kim SH, Park JA, Kim JH, Lee JW, Seo JH, Jung BK, Chun KH, Jeong JW, Bae MK, Kim KW. Characterization of ARD1 variants in mammalian cells. *Biochem. Biophys. Res. Commun* 2006;340(2):422–427. [PubMed: 16376303]

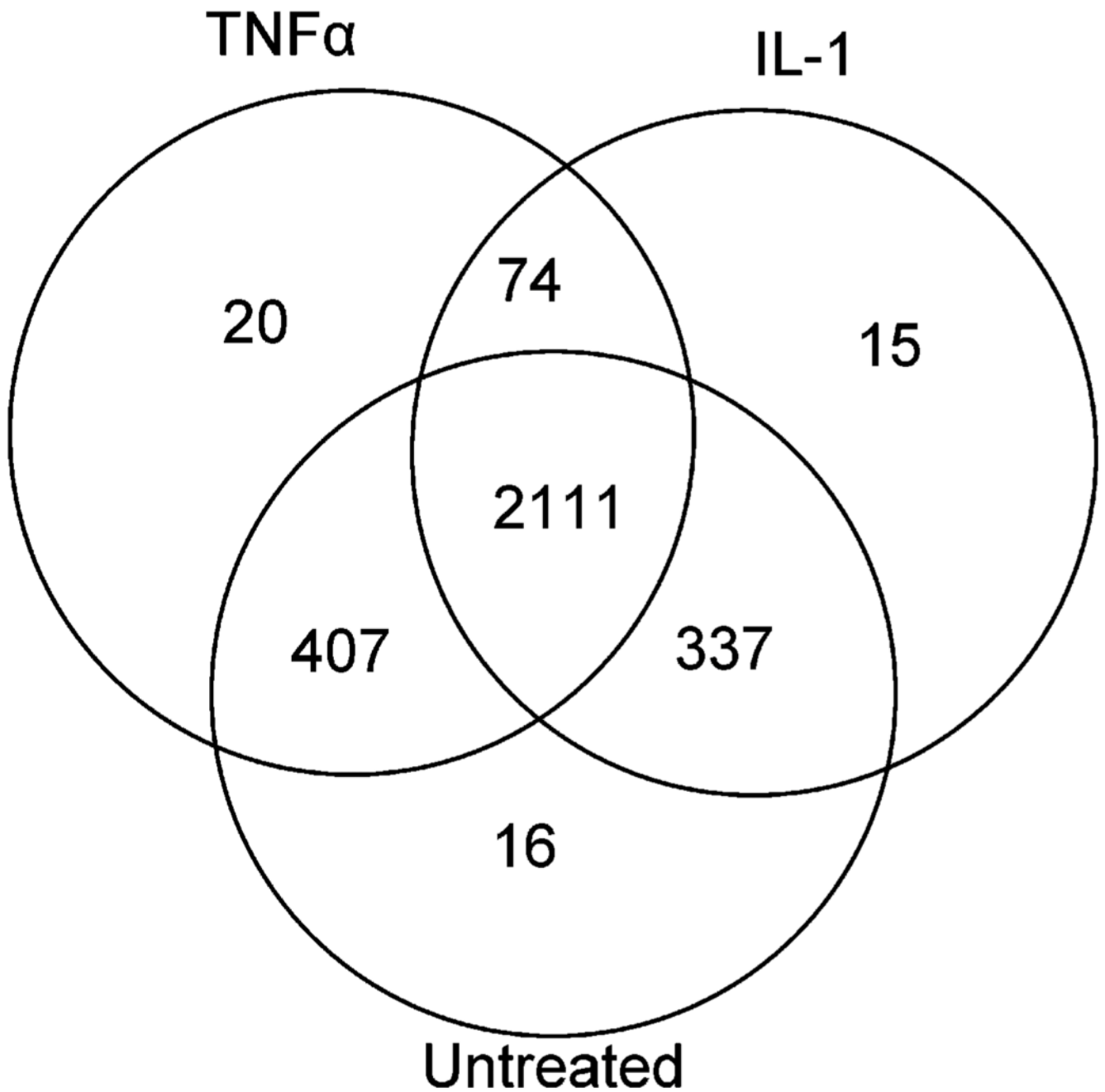


Figure 1.

Euler diagram of all identified proteins after removal of single hit proteins. A total of 2980 proteins remained after excluding single hit proteins. The circles represent the three groups: TNF α -treated, IL-1 treated, or untreated. Circle intersections represent the number of proteins common between two or more of the groups.

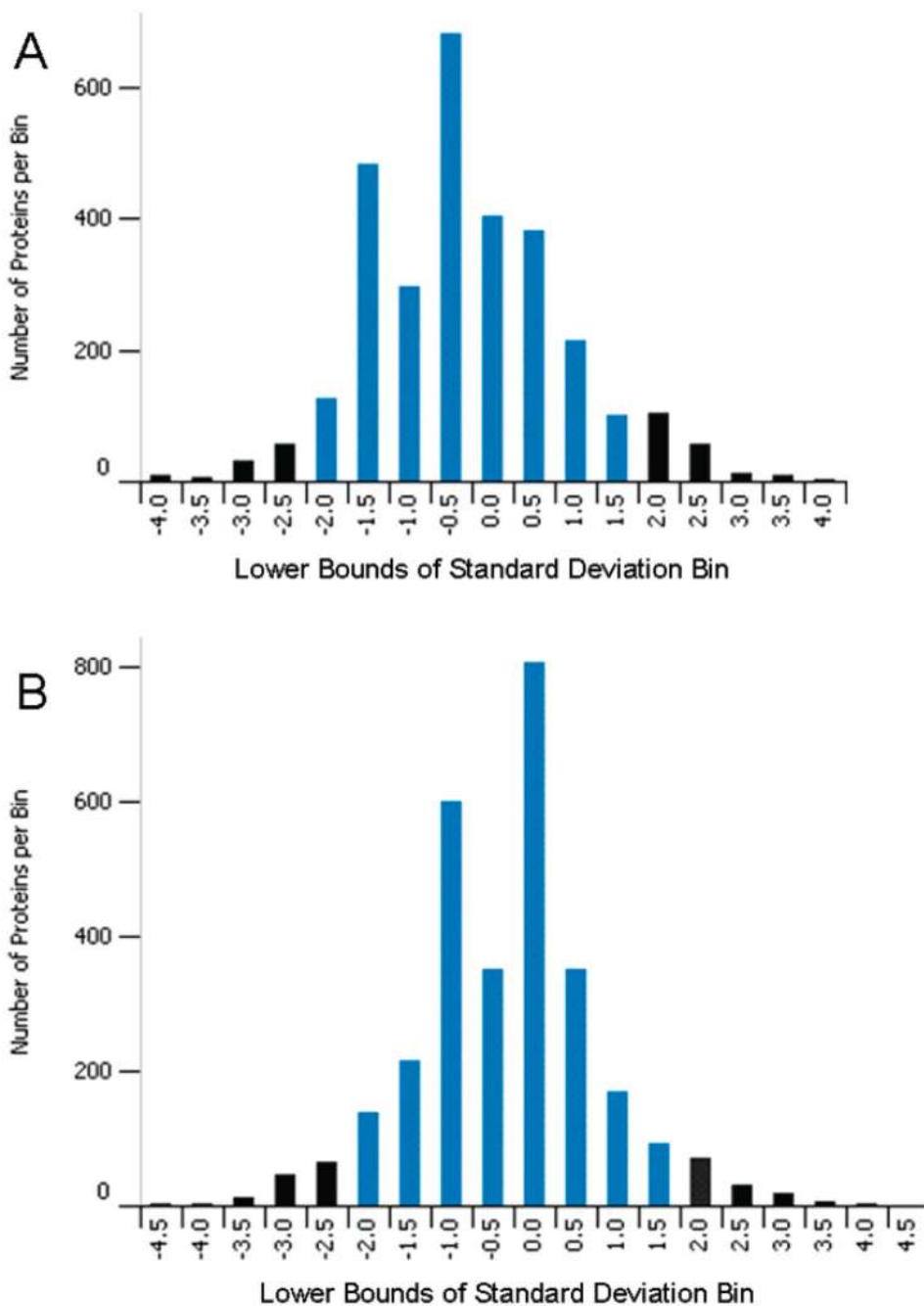
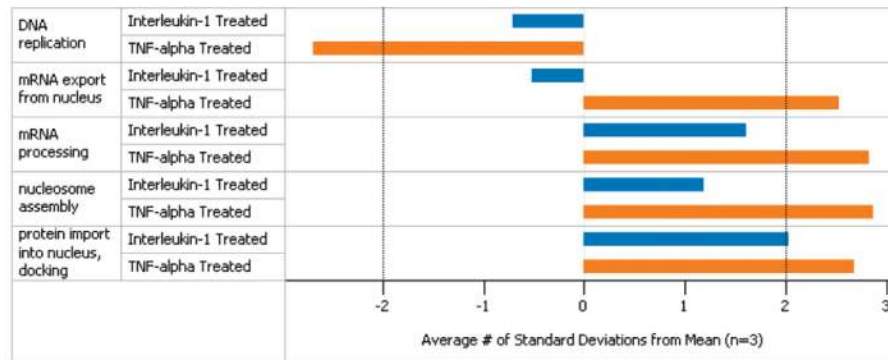


Figure 2. Distribution of protein ratios from TNF α - and IL-1-treated data sets. (A) TNF α - or (B) IL-1-treated versus untreated protein ratios were placed into bins separated by 0.5σ . The total number of proteins for a particular bin is plotted along the y-axis; while the x-axis represents standard deviation bins. Only proteins greater than 2σ away from the sample mean (black bars) were considered for network analysis.

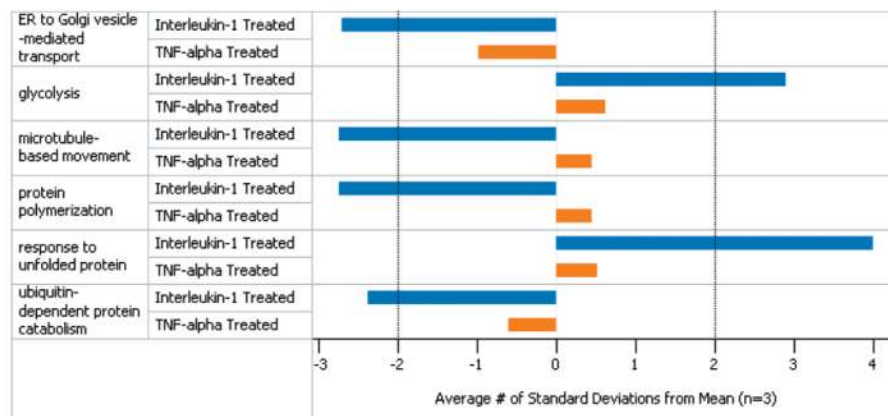
A) TNF Regulated Processes

Nucleus

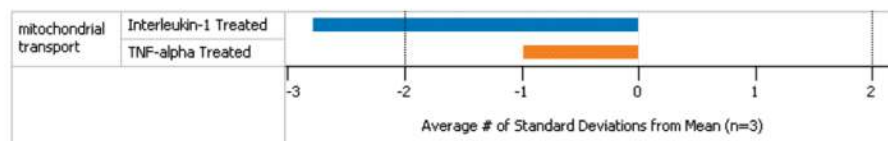


B) IL-1 Regulated Processes

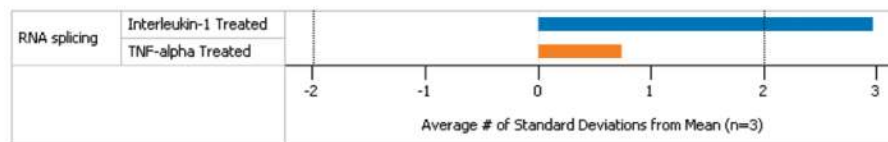
Cytosol



Mitochondrion



Nucleus

**Figure 3.**

GO processes changed significantly in response to TNF α and IL-1 as a function a subcellular compartment. Proteins at least 2σ away from the mean were grouped according to their processes for TNF α - and IL-1-treated cells. Each GO process was then assigned a GO component. The average number of standard deviations from the mean were calculated for each GO process. Only processes $>2\sigma$ were considered significant as indicated by the dotted line.

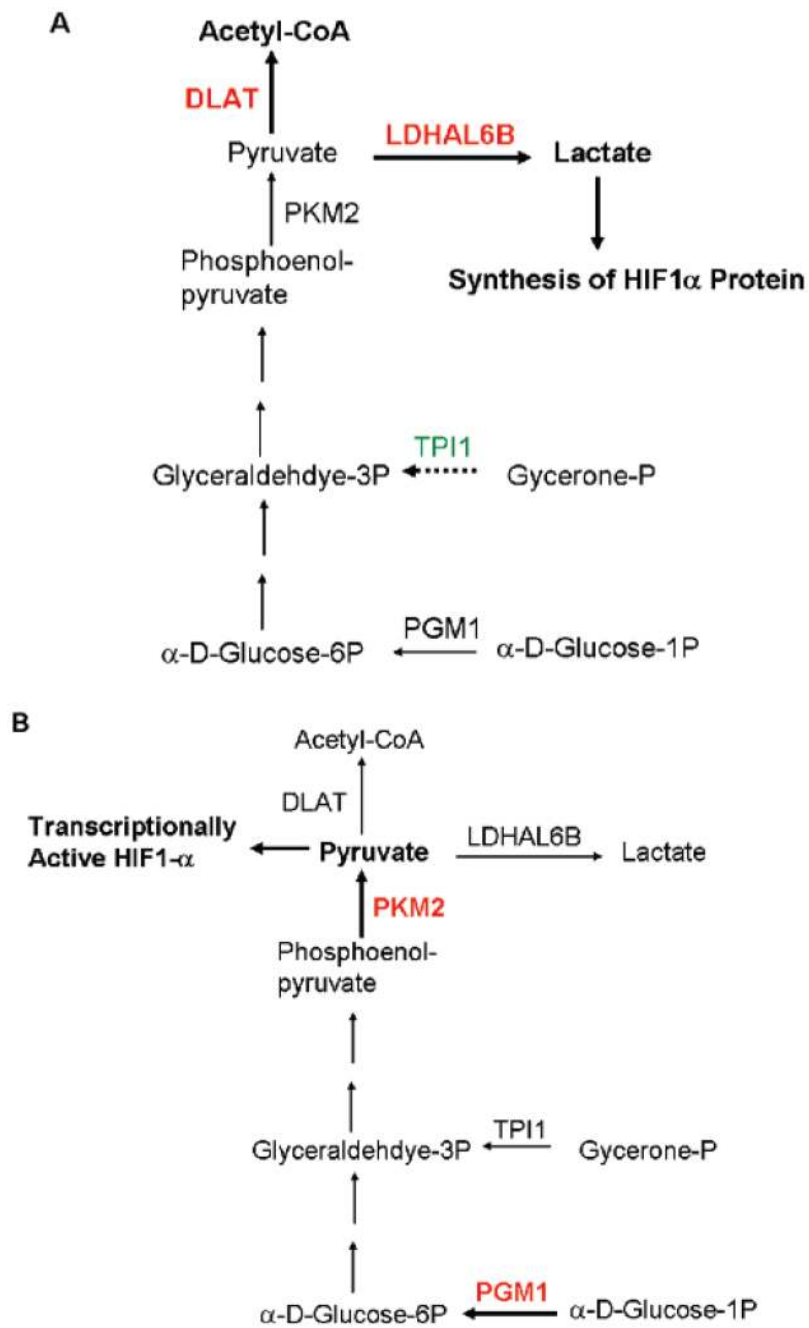


Figure 4.

TNF α and IL-1 regulation of lactate and pyruvate metabolism. (A) TNF α stimulates the production of lactate, which leads to accumulation of HIF1 α protein. (B) IL-1 stimulates the production of pyruvate, which activates the transcription activity of HIF1 α . Proteins increased in response to cytokine treatment are shown in red. Proteins decreased in response to cytokine treatment are shown in green.

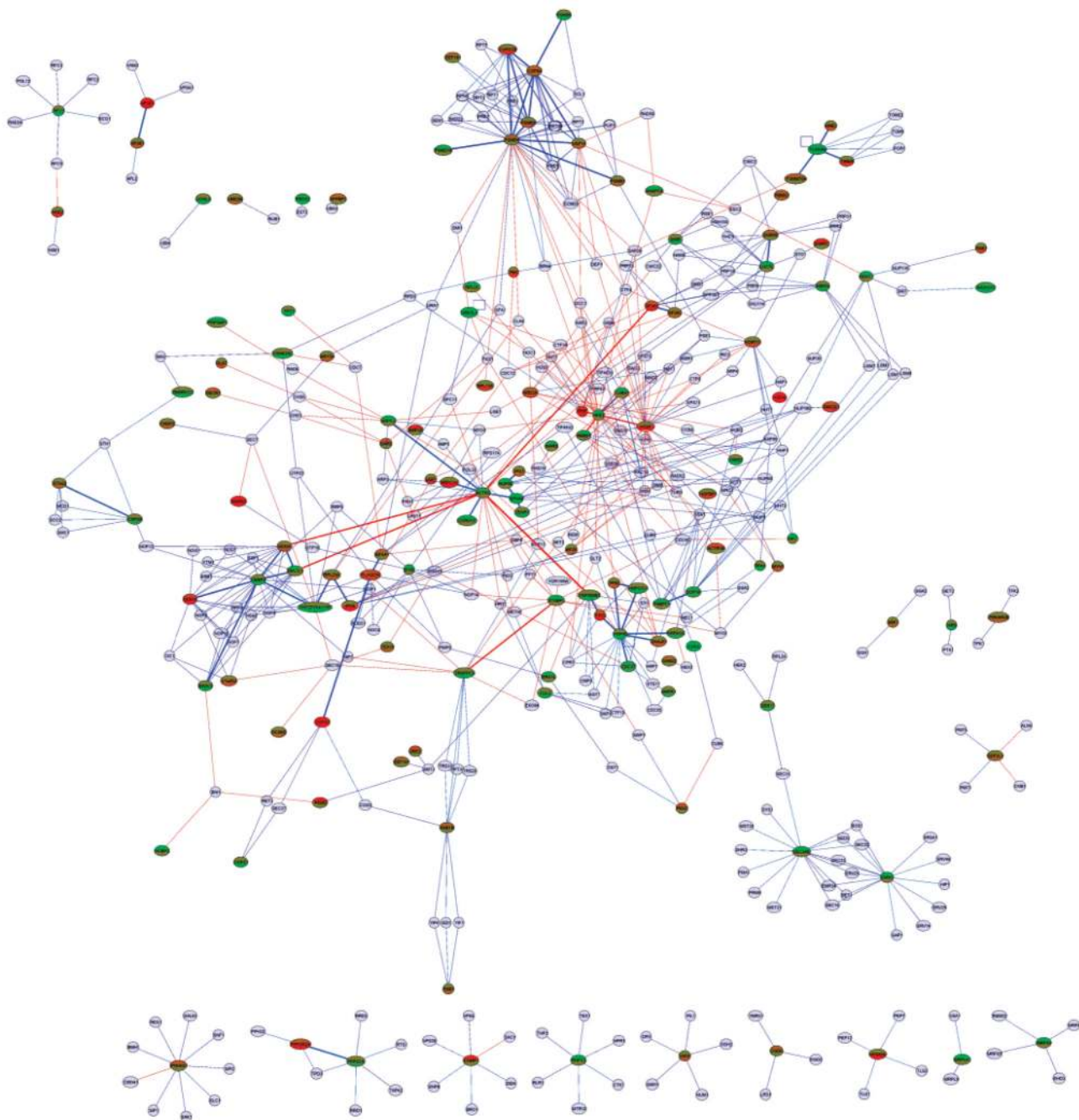


Figure 5. TNF α and IL-1 interaction network. Each node contains two halves, where the top half represents the change seen upon IL-1 treatment, and the bottom half represents the change seen upon TNF α treatment. A color gradient of red (increased protein levels) to green (decreased protein levels) was used to show a particular protein's response to cytokine treatment. These bicolored nodes are labeled with human protein names, while light blue nodes are labeled with yeast protein names and represent proteins with no currently known homologue or no significant change in protein levels. Red edges connecting the nodes represent synthetic lethalities, and the blue edges represent physical interactions resulting from affinity capture

experiments and/or reconstituted complexes. An image (JPG) of the protein interaction network is presented in supplemental Figure S3 in Supporting Information.

Table 1

Relationships between Standard Deviations from the Mean (Z-Score) and Fold Differences in Protein Abundance

	TNFα	IL-1
< -3σ	-3.41 to -3.92	-3.20 to -4.37
-2σ to -3σ	-2.27 to -3.41	-2.17 to -3.20
-1σ to -2σ	-1.51 to -2.27	-1.47 to -2.17
Mean to -1σ	1.01 to -1.51	1.05 to -1.47
Mean to 1σ	1.01 to 1.51	1.05 to 1.47
1σ to 2σ	1.51 to 2.27	1.47 to 2.17
2σ to 3σ	2.27 to 3.41	2.17 to 3.20
$>3\sigma$	3.41 to 6.12	3.20 to 6.78

Table 2Z-Scores for TNF α and interleukin-1 Regulated Proteins and mRNAs^{a,b,c},

Cell Cycle Genes				
Gene	Protein IL-1	mRNA IL-1	Protein TNF α	mRNA TNF α
ARDIA	2.180	-0.340	2.572	-1.209
CCNA1	NA	-0.353	NA	-2.749
CDC37	-2.094	0.527	-2.114	1.879
CDC6	NA	-2.257	NA	-0.506
CDK2	-2.921	-0.080	-2.484	-0.472
CDKN1B	NA	-2.847	NA	0.322
CDKN3	NA	-2.281	NA	-0.167
CUL2	-1.878	-0.309	-2.326	-0.660
PIN1	0.610	NA	2.996	NA
DNA Replication Genes				
Gene	Protein IL-1	mRNA IL-1	Protein TNF α	mRNA TNF α
PCNA	-1.701	-2.293	-2.037	-0.667
RFC2	-1.812	-0.358	-3.638	0.490
RPA1	-0.498	-1.593	-2.326	-1.830
RPA3	-2.512	-0.526	-2.347	-2.622
Mitochondrial Permeability Transition Pore Genes				
Gene	Protein IL-1	mRNA IL-1	Protein TNF α	mRNA TNF α
TIMM9	0.949	-0.703	2.926	-0.421
TOMM40	-2.974	0.325	-2.659	-0.269
PPIF	3.272	0.342	3.405	1.483
Pyruvate and Lactate Metabolism Genes				
Gene	Protein IL-1	mRNA IL-1	Protein TNF α	mRNA TNF α
DLAT	0.512	-1.244	2.509	-0.353
PKM2	3.659	0.314	0.088	-0.221
TPI1	-1.845	0.619	-3.052	-0.678
HIF1-alpha Transcriptional Activity Regulatory Genes				
Gene	Protein IL-1	mRNA IL-1	Protein TNF α	mRNA TNF α
MAPK1	0.511	0.107	-2.121	-0.403
CEBPZ	-0.936	-0.653	-2.326	-0.073

^aRed protein or mRNA levels are T least 2 σ above the mean.^bGreen protein or mRNA levels are least 2 σ below the mean.^cNA indicates genes that were not detected during the indicated analysis.